Journal of Advances in Mathematics and Computer Science

Volume 38, Issue 2, Page 32-47, 2023; Article no.JAMCS.95988
ISSN: 2456-9968
(Past name: British Journal of Mathematics & Computer Science, Past ISSN: 2231-0851)

Effects of Viscosity and Magnetic Field on a Non-Isothermal Cylindrical Channel Flow

Ndu Roseline Ize [a*], Chinedu Nwaigwe [a] and Amos Emeka [a]

[a] *Department of Mathematics, Rivers state University of Science and Technology, Port Harcourt, Nigeria.*

Authors' contributions

This work was carried out in collaboration among all authors. All authors read and approved the final manuscript.

Article Information

DOI: 10.9734/JAMCS/2023/v38i21744

Open Peer Review History:
This journal follows the Advanced Open Peer Review policy. Identity of the Reviewers, Editor(s) and additional Reviewers, peer review comments, different versions of the manuscript, comments of the editors, etc are available here: https://www.sdiarticle5.com/review-history/95988

Original Research Article

Received: 28/10/2022
Accepted: 30/12/2022
Published: 27/01/2023

Abstract

This study examines the effect of viscosity and magnetic field on a non-isothermal cylindrical channel flow. This work considered a model of convective-thermal-diffusion with constant viscosity and magnetic field. The governing model equations are nondimensionalized using the dimensionless quantities and then solved analytically using power series method of Frobenius type so as to tackle the singularity in the model equations. Furthermore, the analytical solutions are displayed via graphs to show the effects of the flow parameters on the flow velocity, temperature and concentration profiles. The graphical results show that increase in viscosity, magnetic field and solutal Grashof number parameters retard the fluid flow. While increase in thermal Grashof number enhances the flow velocity. Thermal conductivity and solute injection parameters increase the fluid temperature and concentration respectively while the cooling and diffusive parameters decrease the fluid temperature and concentration respectively. Further studies can be carried out for a multi-directional flow as against the unidirectional flow and in a vertical channel in place of horizontal channel as studied in this paper.

**Corresponding author: Email: roseline.ndu@ust.edu.ng;*

Keywords: *Cylindrical channel; thermal Grashof; Solutal Grashof; fluid velocity; viscosity; magnetic field; temperature and concentration.*

Nomenclatures

$u^* :=$ *Dimensional velocity components*
$u_0\,(r) :=$ *Dimensionless velocity*
$u(r) :=$ *Velocity profile of the fluid*
$\beta :=$ *coefficient of volumetric expansion*
$\theta_0(r) :=$ *Dimensionless temperature*
$q_r^* :=$ *Radiative heat flux*
$\theta(r) :=$ *Temperature profile*
$\alpha :=$ *Concentration injection parameter*
$C_0(r) :=$ *Dimensionless concentration*
$\lambda :=$ *Temperature cooling parameter*
$C(r) :=$ *Concentration profile*
$\theta_w :=$ *Temperature boundary parameter*
$Gr :=$ *Grashof number*
$T_\infty^* :=$ *Free stream temperature*
$C_w :=$ *Temperature boundary parameter*
$z^* :=$ *Dimensional axisymmetric flow of channel*
$Gr :=$ *Grashof number*
$r^* :=$ *Dimensional radius*
$P :=$ *Pressure gradient*
$t^* :=$ *Dimensional time*
$T^* :=$ *Dimensional fluid temperature*
$T_w^* :=$ *Dimensional wall temperature*
$\rho :=$ *Fluid density*
$M :=$ *Magnetic field parameter*
$k :=$ *Thermal conductivity*
$g :=$ *Acceleration due to gravity*
$\mu :=$ *fluid viscosity*
$\sigma :=$ *Electrical conductivity*
$C_p :=$ *Heat capacity*

1 Introduction

Fluid flow with nonconstant change in temperature is referred to as non-isothermal flow. Such flow has its applications in heat transfer, convection and radiation in solid, porous and surface to surface media. Activities associated to a non-isothermal flow are industrial processes, heat exchangers and coating activities [1]. Several studies have addressed problem on a non-isothermal channel flow [2,3]. For example, a work on non-isothermal flow absorption in a cylindrical tube was investigated and an analytical solution was obtained for mass fraction and temperature distribution within the fluid by Conlisk et al. [4]. Duffy and Wilson [5] examined a two dimensional gravitational driven and viscous-temperature - dependent flow in a heated or cooled stationary horizontal cylinder. While a numerical study on a pressure driven non-isothermal flow was done by Pinarbasi and Imal [6] with a discovery that for a certain range of flow the pressure gradient is monotonic. Adegbie and Alao [7] solved numerically the problem of viscous steady flow in a heated channel so as to investigate the impact of viscosity and viscous dissipation resulting to high rate of flow and discovered that the solution is zero when the viscous heating parameter is zero. Sahu et al. [8] numerically examined a coupled energy and convective-diffusive pressure-driven non-isothermal miscible displacement flow in a viscous heating horizontal channel. Another study on the effect of heat transfer variation and thermoviscosity in and out of the atmosphere layer was displayed by Leslie and coworkers [1].

Using a euler-lagrange approach of modelling Jazcscur [9] carried an investigation in a fully developed non-isotherml flow packed with particles and find out that particle's mean temperature is very much affected with increase in particle concentration near the walls. While Subhakar and others [10] who took into consideration constant viscosity and thermal conductivity of the work of [11]. Furthermore, Nwaigwe & Makinde [12] considered a coupled effect of energy dependent viscosity alongside with specie dependent diffusivity in a non-isothermal pressure driven and unsteady flow. Also, Misyura [13] investigated on a nonisothermal flow in salty solution taking into account the effect of temperature and concentration in the solution. A two-dimensional nonisothermal flow over a square cylinder submerged in a channel was studied by Santos [14], hence, comparing results in terms of Reynold number, drag and lift coefficient values with other researchers to ascertain his numerical computational model. Nwaigwe and coworkers [15] investigated the flow of a thermal radiating fluid with temperature-dependent thermal and constant viscous dissipation. It was realized that increase in the movement of wall channel increases the fluid velocity. While Ahmed and his team [11] worked on the MHD mass transfer on a moving nonisothermal flow considering variable viscosity and thermal conductivity presuming the variation viscosity as inverse linear function of temperature . Nwaigwe [16] numerically carried out a work on mass and heat diffusion in a two parallel stationary walls and discovered that the thermal Grashof number and other parameters increase flow velocity of the fluid.

Bunonyo and Amos [17] also a solved blood related problem in a cylindrical inclined channel with magnetic field and considered the effect of mass transfer in the blood flow to discovered that increase in the magnetic field retards the blood flow velocity. The work of Nwaigwe and Amadi [18] examined an analytical solution to a Newtonian fluid transport problem within a cylinder. Their flow was assumed to be axisymmetric and dominated by the channel axis.

Salahuddin et al. [19] worked on the heat and mass transfer incorporating induced magnetic field in an incompressible Williamson fluid having variable thermo-physical properties such as viscosity.

The purpose of this work is to extend the work Nwaigwe and Amadi [18] by infusing a specie concentration, constant viscosity, thermal conductivity and mass diffusive parameter to the fluid in the cylindrical channel. The dimensional and nondimensionless model equations are presented in section 2 and similar method of solution in the extended work is used to tackle singularity in the model section 3. While the graphical results and discussed are displayed in section 4 with conclusion in section 5.

2 Mathematical Formulation

An incomprehensible Newtonian flow of a viscous fluid is assumed to be in a horizontal cylindrical duct in the $\left(r^*, \theta^*, z^*\right)$ coordinates. The flow is considered to be unidirectional only along the z^* −axis with no variation along that axis that is ($u^* = 0$ on $r^* = 1$). The fluid is viscous with no- slip condition effect. The walls of the channels are stationary. The fluid velocity, temperature and concentration are u^*, T^*, C^*. Below is the diagram of the fluid flow, assuming r^* to be the distance from the centre of the channel towards the wall and $\vec{u}^* = (0, 0, u^*)$ is the velocity vector.

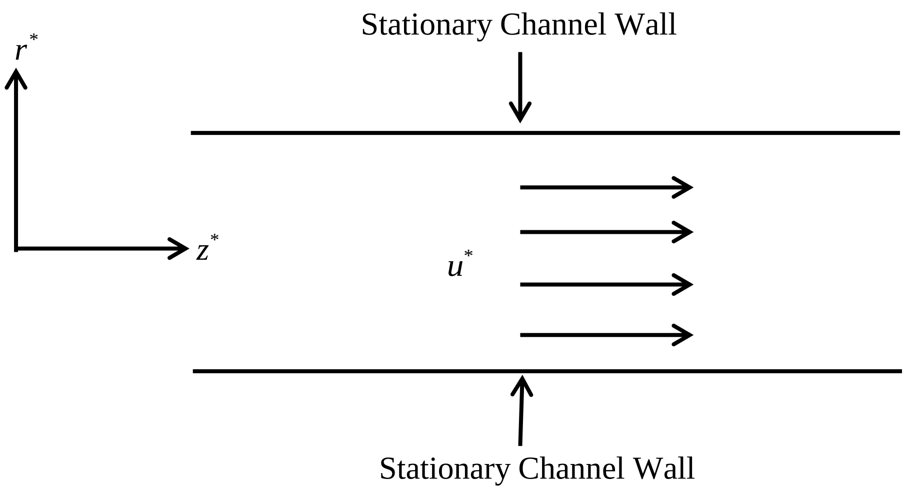

Fig. 1. Physical Representation of the Channel Flow

Further, we assume that, the flow is axi-symmetric, convective-thermal-diffusive with a constant viscosity. The flow is also assumed to be steady and fully developed with a constant pressure gradient.

2.1 Momentum Equation

$$\frac{\partial u_z^*}{\partial z^*} = 0 \tag{1}$$

$$-\frac{\partial P^*}{\rho \partial z^*}+\mu_f\left(\frac{1}{r^*}\frac{\partial}{\partial r^*}\left(r^*\frac{\partial u_z^*}{\partial r^*}\right)\right)+g\beta_T\left(T^*-T_\infty^*\right)-g\beta_C\left(C^*-C_\infty^*\right)-\frac{\sigma B_0^2 u_z^*}{\rho}=0 \tag{2}$$

2.2 Energy equation

$$\kappa^*\left(\frac{1}{r^*}\frac{\partial}{\partial r^*}\left(r^*\frac{\partial T^*}{\partial r^*}\right)\right)-Q_0\left(T^*-T_\infty^*\right)=0 \tag{3}$$

2.3 Mass concentration equation

$$D_0\left(\frac{1}{r^*}\frac{\partial}{\partial r^*}\left(r^*\frac{\partial C^*}{\partial r^*}\right)\right)+Q_1\left(C^*-C_\infty^*\right)=0 \tag{4}$$

The corresponding boundary conditions are

$$\left.\begin{array}{ll}\frac{du^*}{dr^*}=0,\frac{dT^*}{dr^*}=0,\frac{dC^*}{dr^*}=0 & \text{at } r^*=0\\ u^*=0,T^*=T_w^*,\mathrm{C}^*=C_w^* & \text{at } r^*=1\end{array}\right\} \tag{5}$$

Where u^* is the fluid velocity component along z^* direction, μ_f is the viscosity, ρ is the density of the fluid, g .
is the acceleration due to gravity, β_T is the volumetric expansion coefficient for temperature, T^* .
is the fluid temperature, T_∞^* is the free stream temperature, β_c is the volumetric expansion coefficient for concentration, C^* is the fluid concentration, C_∞^* is the free stream concentration, σ is the electrical conductivity of the fluid. B_0^2 is the uniform magnetic intensity, κ^* is the fluid thermal conductivity.

2.4 Dimensionless parameters

$$\left.\begin{array}{l}\theta=\frac{T^*-T_\infty^*}{T_w^*},C=\frac{C^*-C_\infty^*}{C_w^*},Gr=\frac{g\beta_T T_w^* a^2}{\upsilon_0^2},Gc=\frac{g\beta_C C_w^* a^2}{\upsilon_0^2},\lambda^2=\frac{Q_0 a^2}{\kappa_0},\\ z=\frac{z^*}{a},r=\frac{r^*}{a},u=\frac{u_z^* a}{\upsilon_0},P=\frac{a^2P^*}{\rho\upsilon_0^2},M=B_0 a\sqrt{\frac{\sigma_e}{\mu_0}},C_w=1-\frac{C_\infty^*}{C_w^*},\alpha^2=\frac{Q_1 a^2}{D_0}\\ \mu=\frac{\mu_f}{\mu_0},\theta_w=1-\frac{T_\infty^*}{T_w^*},\kappa=\frac{\kappa^*}{\kappa_0},D=\frac{D_0}{D^*},p=-\frac{\partial P}{\partial z}\end{array}\right\} \tag{6}$$

The dimensionless parameters in equation (6) are applied to give the dimensionless governing equations as follow:

$$\mu\left(\frac{\partial^2 u}{\partial r^2}+\frac{1}{r}\frac{\partial u}{\partial r}\right)-M^2u=p-\theta Gr+CGc \tag{7}$$

$$\kappa\left(\frac{\partial^2\theta}{\partial r^2}+\frac{1}{r}\frac{\partial\theta}{\partial r}\right)-\lambda^2\theta=0 \tag{8}$$

$$D\left(\frac{\partial^2 C}{\partial r^2}+\frac{1}{r}\frac{\partial C}{\partial r}\right)+\alpha^2 C=0 \tag{9}$$

The corresponding boundary conditions:

$$\left.\begin{array}{ll}\frac{\partial u}{\partial r}=0,\frac{\partial\theta}{\partial r}=0,\frac{\partial C}{\partial r}=0 & \text{at } r=0\\ u=0,\theta=\theta_w,C=C_w & \text{at } r=1\end{array}\right\} \tag{10}$$

where μ is the viscous term, κ is the thermal conductivity, D is the diffusive term, p is the pressure term, M is the magnetic field parameter, α is the injection term, λ is the cooling term, Gr is the thermal Grashof number and Gc is the solutal Grashof number.

Since u is a function of r only, the system of ordinary of differential equations are obtained as below :

$$\mu\left(\frac{d^2u}{dr^2}+\frac{1}{r}\frac{du}{dr}\right)-M^2u=p-\theta Gr+CGc \tag{11}$$

$$\kappa\left(\frac{d^2\theta}{dr^2}+\frac{1}{r}\frac{d\theta}{dr}\right)-\lambda^2\theta=0 \tag{12}$$

$$D\left(\frac{d^2C}{dr^2}+\frac{1}{r}\frac{dC}{dr}\right)+\alpha^2C=0 \tag{13}$$

The corresponding boundary conditions:

$$\left.\begin{array}{ll}\frac{du}{dr}=0,\frac{d\theta}{dr}=0,\frac{dC}{dr}=0 & \text{at } r=0\\ u=0,\theta=\theta_w,C=C_w & \text{at } r=1\end{array}\right\} \tag{14}$$

3 Method of Solution

To solve equations (11), (12),(13) and (14), unique solutions of the forms are assumed below:

$$u(r)=A_0u_0(r)+A_1u_1(r) \tag{15}$$

$$\theta(r)=A_2\theta_0(r)+A_3\theta_1(r) \tag{16}$$

$$C(r)=A_4C_0(r)+A_5C_1(r) \tag{17}$$

where $u_0(r)$, $u_1(r)$, $\theta_0(r)$, $\theta_1(r)$, $C_0(r)$ and $C_1(r)$ are two linearly independent solutions with A_0, A_1, A_2, A_3, A_4 and A_5 as arbitrary constants. Hence, to obtain $u_0(r)$, $\theta_0(r)$ and $C_0(r)$, a power series solution of Frobenius type is employed as follow: (see Nwaigwe and Amadi [15]).

$$u_0\left(r\right)=\sum_{p=0}^{\infty}a_p r^{p+m}; \tag{18}$$

$$\theta_0\left(r\right)=\sum_{p=0}^{\infty}\dot{a}_p r^{p+m}; \tag{19}$$

$$C_0\left(r\right)=\sum_{p=0}^{\infty}\ddot{a}_p r^{p+m}; \qquad m=\text{constant} \tag{20}$$

where $a_p, \dot{a}_p$, and $\ddot{a}_p$ are constants to be determined.

To solve for equations (11) – (13), equations (18) – (20) are first differentiated twice and substituted into equations (11) - (13) to obtain :

$$u_0\left(r\right)=r^m\left(\begin{array}{l} a_0+\left(\dfrac{M^2a_0}{(m+2)^2\mu}\right)r^2+\left(\dfrac{M^2a_2}{(m+4)^2\mu}\right)r^4+\left(\dfrac{M^2a_4}{(m+6)^2\mu}\right)r^6-\left(\dfrac{\alpha^2a_6}{(m+8)^2\mu}\right)r^8\\ +\left(\dfrac{M^2a_8}{(m+10)^2\mu}\right)r^{10}+\ldots\end{array}\right) \tag{21}$$

$$\theta_0\left(r\right)=r^m\left(\begin{array}{l} \dot{a}_0+\left(\dfrac{\lambda^2\dot{a}_0}{(m+2)^2\kappa}\right)r^2+\left(\dfrac{\lambda^2\dot{a}_2}{(m+4)^2\kappa}\right)r^4+\left(\dfrac{\lambda^2\dot{a}_4}{(m+6)^2\kappa}\right)r^6-\left(\dfrac{\alpha^2\dot{a}_6}{(m+8)^2\kappa}\right)r^8\\ +\left(\dfrac{\lambda^2\dot{a}_8}{(m+10)^2\kappa}\right)r^{10}+\ldots\end{array}\right) \tag{22}$$

$$C_0\left(r\right)=r^m\left(\begin{array}{l} \ddot{a}_0-\left(\dfrac{\alpha^2\ddot{a}_0}{(m+2)^2D}\right)r^2-\left(\dfrac{\alpha^2\ddot{a}_2}{(m+4)^2D}\right)r^4-\left(\dfrac{\alpha^2\ddot{a}_4}{(m+6)^2D}\right)r^6-\left(\dfrac{\alpha^2\ddot{a}_6}{(m+8)^2D}\right)r^8\\ -\left(\dfrac{\alpha^2\ddot{a}_8}{(m+10)^2D}\right)r^{10}+\ldots\end{array}\right) \tag{23}$$

where the even values $a_{p's}$ are only displayed, leaving out the odd values $a_{(p+1)'s}$ since they are all zeros. Therefore rewriting equations (21), (22) and (23) in terms of a_0, the results are shown as :

$$u_0(r)=r^m\left(\begin{array}{l}\left(a_0-\frac{(Mr)^2a_0}{D(m+2)^2}+\left(\frac{(Mr)^4a_0}{D^2(m+2)^2(m+4)^2}\right)-\left(\frac{(Mr)^6a_0}{D^3(m+2)^2(m+4)^2(m+6)^2}\right)\right.\\ \left.+\left(\frac{(Mr)^8a_0}{D^4(m+2)^2(m+4)^2(m+6)^2(m+8)^2}\right)-\left(\frac{(Mr)^{10}a_0}{D^5(m+2)^2(m+4)^2(m+6)^2(m+8)^2(m+10)^2}\right)+\ldots\right)\end{array}\right) \quad (24)$$

$$\theta_0(r)=r^m\left(\begin{array}{l}\left(\dot{a}_0+\frac{(\alpha r)^2\dot{a}_0}{D(m+2)^2}+\left(\frac{(\alpha r)^4\dot{a}_0}{D^2(m+2)^2(m+4)^2}\right)+\left(\frac{(\alpha r)^6\dot{a}_0}{D^3(m+2)^2(m+4)^2(m+6)^2}\right)\right.\\ \left.+\left(\frac{(\alpha r)^8\dot{a}_0}{D^4(m+2)^2(m+4)^2(m+6)^2(m+8)^2}\right)+\left(\frac{(\alpha r)^{10}\dot{a}_0}{D^5(m+2)^2(m+4)^2(m+6)^2(m+8)^2(m+10)^2}\right)+\ldots\right)\end{array}\right) \quad (25)$$

$$C_0(r)=r^m\left(\begin{array}{l}\left(\ddot{a}_0-\frac{(\alpha r)^2\ddot{a}_0}{D(m+2)^2}+\left(\frac{(\alpha r)^4\ddot{a}_0}{D^2(m+2)^2(m+4)^2}\right)-\left(\frac{(\alpha r)^6\ddot{a}_0}{D^3(m+2)^2(m+4)^2(m+6)^2}\right)\right.\\ \left.+\left(\frac{(\alpha r)^8\ddot{a}_0}{D^4(m+2)^2(m+4)^2(m+6)^2(m+8)^2}\right)-\left(\frac{(\alpha r)^{10}\ddot{a}_0}{D^5(m+2)^2(m+4)^2(m+6)^2(m+8)^2(m+10)^2}\right)+\ldots\right)\end{array}\right) \quad (26)$$

To obtain $u_1(r)$, $\theta_1(r)$ and $C_1(r)$ in equations (15) – (17), equations (24), (25) and (26) are differentiated with respect to m to obtain:

$$u_1(r)=\frac{\partial u_0(r)}{\partial m}=\left[\begin{array}{l}a_0r^m\ln r\left(\begin{array}{l}1+\frac{(Mr)^2}{\mu(m+2)^2}+\frac{(Mr)^4}{\mu^2(m+2)^2(m+4)^2}+\frac{(Mr)^6}{\mu^3(m+2)^2(m+4)^2(m+6)^2}\\ +\frac{(Mr)^8}{\mu^4(m+2)^2(m+4)^2(m+6)^2(m+8)^2}+\frac{(Mr)^{10}}{\mu^5(m+2)^2(m+4)^2(m+6)^2(m+8)^2(m+10)^2}\end{array}\right)\\ -\frac{2(\alpha r)^2}{\mu}a_0r^m\left(\begin{array}{l}\frac{1}{(m+2)^3}+\frac{2(Mr)^2(m+3)}{\mu(m+2)^3(m+4)^3}+\frac{(Mr)^4(44+3m(m+8))}{\mu^2(m+2)^3(m+4)^3(m+6)^3}\\ +\frac{4(Mr)^6(100+m(m^2+15m+70))}{\mu^3(m+2)^3(m+4)^3(m+6)^3(m+8)^3}+\frac{(Mr)^8(4384+5m(m^3+24m^2+204m+720))}{\mu^4(m+2)^3(m+4)^3(m+6)^3(m+8)^3(m+10)^3}\end{array}\right)\end{array}\right] \quad (27)$$

$$\theta_1(r)=\frac{\partial \theta_0(r)}{\partial m}=\left[\begin{array}{l}a_0r^m\ln r\left(\begin{array}{l}1+\frac{(\lambda r)^2}{\kappa(m+2)^2}+\frac{(\lambda r)^4}{\kappa^2(m+2)^2(m+4)^2}+\frac{(\lambda r)^6}{\kappa^3(m+2)^2(m+4)^2(m+6)^2}\\ +\frac{(\lambda r)^8}{\kappa^4(m+2)^2(m+4)^2(m+6)^2(m+8)^2}+\frac{(\lambda r)^{10}}{\kappa^5(m+2)^2(m+4)^2(m+6)^2(m+8)^2(m+10)^2}\end{array}\right)\\ -\frac{2(\lambda r)^2}{\kappa}a_0r^m\left(\begin{array}{l}\frac{1}{(m+2)^3}+\frac{2(\lambda r)^2(m+3)}{\kappa(m+2)^3(m+4)^3}+\frac{(\lambda r)^4(44+3m(m+8))}{\kappa^2(m+2)^3(m+4)^3(m+6)^3}\\ +\frac{4(\lambda r)^6(100+m(m^2+15m+70))}{\kappa^3(m+2)^3(m+4)^3(m+6)^3(m+8)^3}+\frac{(\lambda r)^8(4384+5m(m^3+24m^2+204m+720))}{\kappa^4(m+2)^3(m+4)^3(m+6)^3(m+8)^3(m+10)^3}\end{array}\right)\end{array}\right] \quad (28)$$

$$C_1(r)=\frac{\partial C_0(r)}{\partial m}=\left[\begin{array}{l} \ddot{a}_0 r^m \ln r\left(\begin{array}{l} 1-\frac{(\alpha r)^2}{D(m+2)^2}+\frac{(\alpha r)^4}{D^2(m+2)^2(m+4)^2}-\frac{(\alpha r)^6}{D^3(m+2)^2(m+4)^2(m+6)^2} \\ +\frac{(\alpha r)^8}{D^4(m+2)^2(m+4)^2(m+6)^2(m+8)^2}-\frac{(\alpha r)^{10}}{D^5(m+2)^2(m+4)^2(m+6)^2(m+8)^2(m+10)^2} \end{array}\right) \\ +\frac{2(\alpha r)^2}{D}\ddot{a}_0 r^m\left(\begin{array}{l} \frac{1}{(m+2)^3}-\frac{2(\alpha r)^2(m+3)}{D(m+2)^3(m+4)^3}+\frac{(\alpha r)^4(44+3m(m+8))}{D^2(m+2)^3(m+4)^3(m+6)^3} \\ -\frac{4(\alpha r)^6(100+m(m^2+15m+70))}{D^3(m+2)^3(m+4)^3(m+6)^3(m+8)^3}+\frac{(\alpha r)^8(4384+5m(m^3+24m^2+204m+720))}{D^4(m+2)^3(m+4)^3(m+6)^3(m+8)^3(m+10)^3} \end{array}\right) \end{array}\right] \tag{29}$$

Hence, for $m=0$ in equations (21) – (29) taking along the arbitrary constants in equation (15) – (17) the unique solutions for velocity, temperature and concentration are expressed as:

$$u(r)=A_1\left(\begin{array}{l} 1+\frac{(Mr)^2}{2^2\mu}+\left(\frac{(Mr)^4}{(2.4.\mu)^2}\right) \\ +\left(\frac{(Mr)^6}{(2.4.6)^2\mu^3}\right)+\left(\frac{(Mr)^8}{(2.4.6.8)^2\mu^4}\right) \\ +\left(\frac{(Mr)^{10}}{(2.4.6.8.10)^2\mu^5}\right)+\ldots \end{array}\right)+A_2\left[\begin{array}{l} \ln r\left(\begin{array}{l} 1+\frac{(Mr)^2}{2^2\mu}+\frac{(Mr)^4}{2^2.4^2.\mu^2}+\frac{(Mr)^6}{2^2.4^2.6^2\mu^3} \\ +\frac{(Mr)^8}{2^2.4^2.6^2.8^2\mu^4}+\left(\frac{(Mr)^{10}}{(2.4.6.8.10)^2 D^5}\right) \end{array}\right) \\ -\frac{2(Mr)^2}{2^3.\mu}\left(1+\frac{6(Mr)^2}{4^3.\mu}+\frac{44(Mr)^4}{4^3.6^3\mu^2}+\frac{100(Mr)^6}{4^3.6^3.8^3\mu^3}+\frac{4384(Mr)^8}{4^3.6^3.8^3.10^3\mu^4}\right) \end{array}\right]$$
$$+\left(B_0+B_1r+B_2r^2+B_3r^3+B_4r^4+B_5r^5+B_6r^6+B_7r^7+B_8r^8+B_9r^9+B_{10}r^{10}\right) \tag{30}$$

$$\theta(r)=A_2\left(\begin{array}{l} 1+\frac{(\lambda r)^2}{2^2\kappa}+\left(\frac{(\lambda r)^4}{(2.4.\kappa)^2}\right)+\left(\frac{(\lambda r)^6}{(2.4.6)^2\kappa^3}\right) \\ +\left(\frac{(\lambda r)^8}{(2.4.6.8)^2\kappa^4}\right)+\left(\frac{(\lambda r)^{10}}{(2.4.6.8.10)^2\kappa^5}\right)+\ldots \end{array}\right)+A_3\left[\begin{array}{l} \ln r\left(1+\frac{(\lambda r)^2}{2^2\kappa}+\frac{(\lambda r)^4}{2^2.4^2.\kappa^2}+\frac{(\lambda r)^6}{2^2.4^2.6^2\kappa^3}+\frac{(\lambda r)^8}{2^2.4^2.6^2.8^2\kappa^4}+\left(\frac{(\lambda r)^{10}}{(2.4.6.8.10)^2\kappa^5}\right)\right) \\ -\frac{2(\alpha r)^2}{\kappa}\left(\frac{1}{2^3}+\frac{6(\lambda r)^2}{2^3.4^3.\kappa}+\frac{44(\lambda r)^4}{2^3.4^3.6^3\kappa^2}+\frac{100(\lambda r)^6}{2^3.4^3.6^3.8^3\kappa^3}+\frac{4384(\lambda r)^8}{2^3.4^3.6^3.8^3.10^3\kappa^4}\right) \end{array}\right] \tag{31}$$

$$C(r)=A_4\left(\begin{array}{l} 1-\frac{(\alpha r)^2}{2^2D}+\left(\frac{(\alpha r)^4}{(2.4.D)^2}\right)-\left(\frac{(\alpha r)^6}{(2.4.6)^2D^3}\right) \\ +\left(\frac{(\alpha r)^8}{(2.4.6.8)^2D^4}\right)-\left(\frac{(\alpha r)^{10}}{(2.4.6.8.10)^2D^5}\right)+\ldots \end{array}\right)+A_5\left[\begin{array}{l} \ln r\left(1-\frac{(\alpha r)^2}{2^2D}+\frac{(\alpha r)^4}{2^2.4^2.D^2}-\frac{(\alpha r)^6}{2^2.4^2.6^2D^3}+\frac{(\alpha r)^8}{2^2.4^2.6^2.8^2D^4}-\left(\frac{(\alpha r)^{10}}{(2.4.6.8.10)^2D^5}\right)\right) \\ +\frac{2(\alpha r)^2}{D}\left(\frac{1}{2^3}-\frac{6(\alpha r)^2}{2^3.4^3.D}+\frac{44(\alpha r)^4}{2^3.4^3.6^3D^2}-\frac{100(\alpha r)^6}{2^3.4^3.6^3.8^3D^3}+\frac{4384(\alpha r)^8}{2^3.4^3.6^3.8^3.10^3D^4}\right) \end{array}\right] \tag{32}$$

where $B_1=B_3=B_5=B_7=B_9=0$.

Applying boundary conditions in equation (14) to equations (30) – (32) and setting $A_1=A_3=A_5=0$ due to boundedness the following results are obtained:

$$u(r)=\left(\begin{array}{l}A_0+B_0+\left(\dfrac{M^2A_4}{2^2\mu}+B_2\right)r^2+\left(\dfrac{M^4A_0}{(2.4)^2.\mu^2}+B_4\right)r^4+\left(\dfrac{M^6A_0}{(2.4.6)^2\mu^3}+B_6\right)r^6\\+\left(\dfrac{M^8A_0}{(2.4.6.8)^2\mu^4}+B_8\right)r^8+\left(\dfrac{M^{10}A_0}{(2.4.6.8.10)^2\mu^5}+B_{10}\right)r^{10}+\dots\end{array}\right) \tag{33}$$

$$\theta(r)=\frac{\theta_w}{\theta_0(1)}\left(1+\frac{(\lambda r)^2}{2^2\kappa}+\left(\frac{(\lambda r)^4}{(2.4.\kappa)^2}\right)+\left(\frac{(\lambda r)^6}{(2.4.6)^2\kappa^3}\right)+\left(\frac{(\lambda r)^8}{(2.4.6.8)^2\kappa^4}\right)+\left(\frac{(\lambda r)^{10}}{(2.4.6.8.10)^2\kappa^5}\right)+\dots\right) \tag{34}$$

$$C(r)=\frac{C_w}{C_0(1)}\left(1-\frac{(\alpha r)^2}{2^2D}+\left(\frac{(\alpha r)^4}{(2.4.D)^2}\right)-\left(\frac{(\alpha r)^6}{(2.4.6)^2D^3}\right)+\left(\frac{(\alpha r)^8}{(2.4.6.8)^2D^4}\right)-\left(\frac{(\alpha r)^{10}}{(2.4.6.8.10)^2D^5}\right)+\dots\right) \tag{35}$$

4 Results

The graphical results of the analytical solutions for flow velocity, energy and mass concentration are presented in this section varying different parameters such as viscosity,thermal Grashof, solutal Grashof, magnetic field, thermal conductivity, heat source, solute injection and diffusivity.

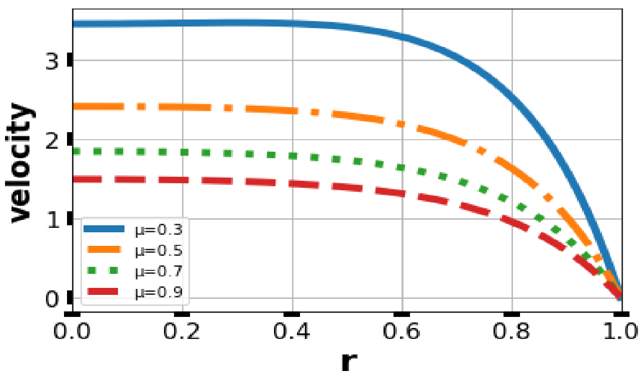

Fig. 2. Velocity Profile against r for the values of Gc=0.5, Gr=0.5,α=0.6,κ=0.3.D=5,M=5, λ=6, P=1.0, varying viscosity parameter

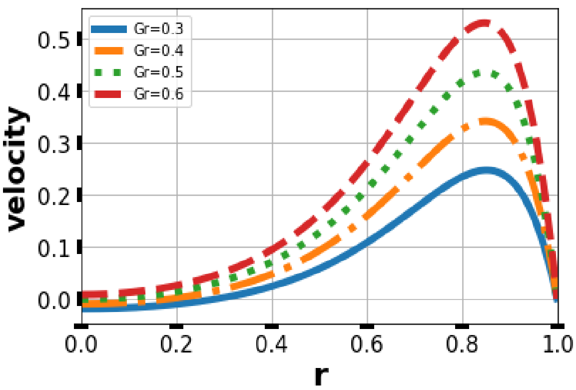

Fig. 3. Velocity Profile against r for the values of Gc=0.5,α=0.6,κ=0.3.D=5,M=6, μ=0.1, λ=3, P=1.0, varying Thermal Grashof Number

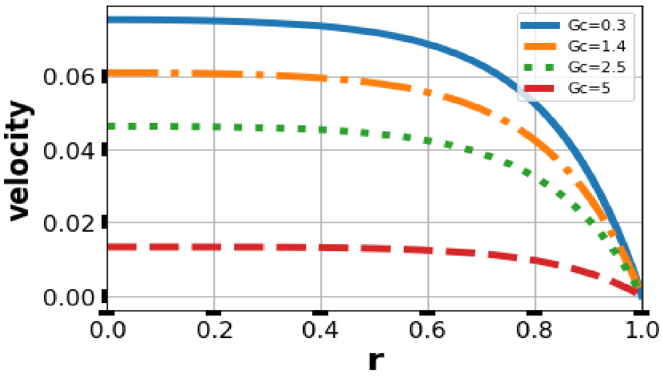

Fig. 4. Velocity Profile against r for the values of Gr=0.5,α=0.6,κ=0.3.D=5,M=6, μ=0.1, λ=0.2, P=1.0, varying solutal Grahof Number

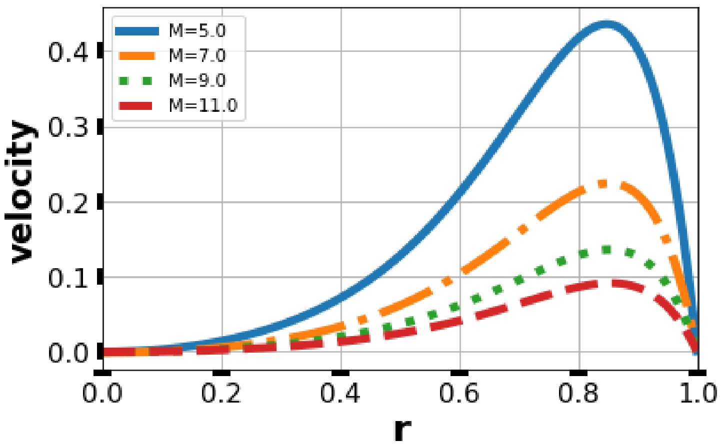

Fig. 5. Velocity Profile against r for the values of Gc=0.5, Gr=0.5, α=0.6, κ=0.3, D=5, μ=0.1, λ=3, P=1.0, varying magnetic field parameter

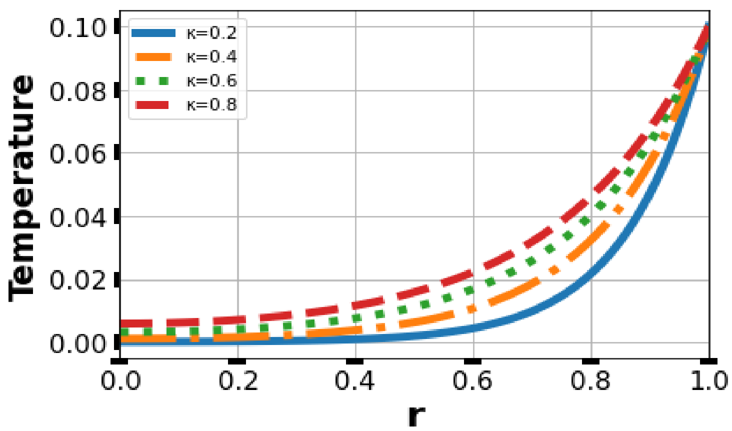

Fig. 6. Temperature Profile against r for the values of θw = 0.1, λ= 4 varying thermal conductivity parameter

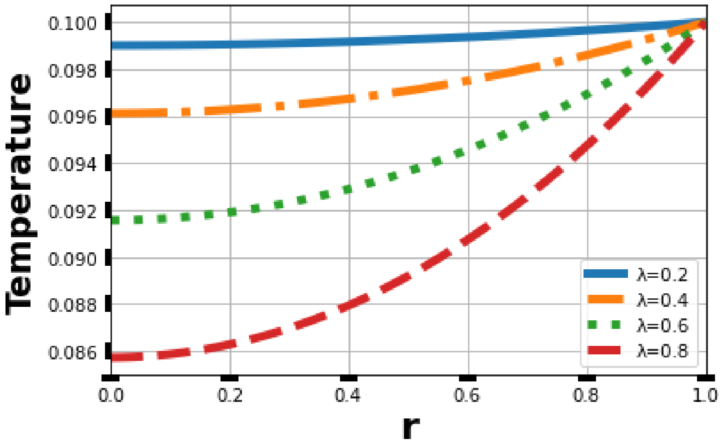

Fig. 7. Temperature Profile against r for the values of θw = 0.1, κ = 1.0 varying heat source parameter

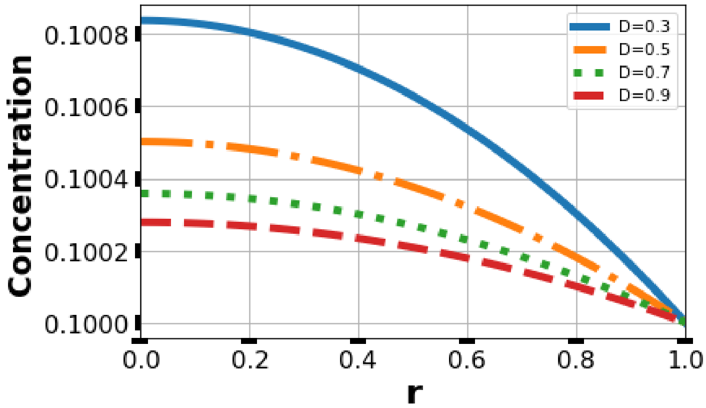

Fig. 8. Concentration Profile against r for the values of Cw = 0.1, α = 1.0, D=1.0, varying Diffusive parameter.

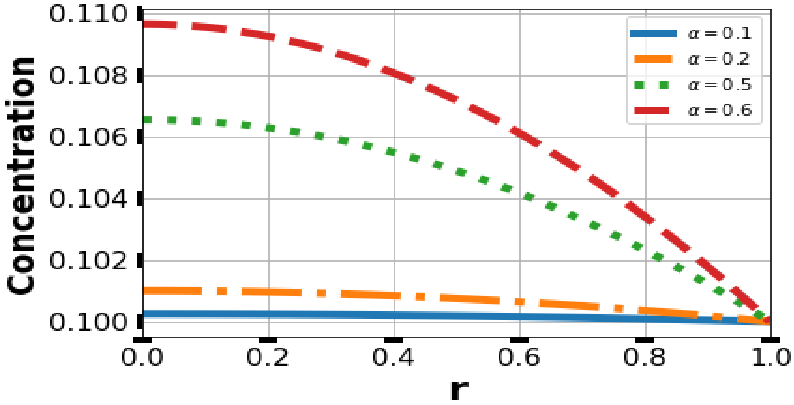

Fig. 9. Concentration Profile against r for the values of Cw = 0.1, D = 1.0 varying solute injection parameter

5 Discussion

Having displayed the graphical results in section 4, the discussions for each graph is shown below:

In Fig. 2, the effect of viscosity parameter on flow velocity is shown. The result depicts that, flow velocity decreases as the viscous parameter increases. This is due to the that fact that there is always flow resistance at the wall of flow as a result of no slip between the wall and the fluid.

Since Thermal Grashof determines the flow regime of a boundary layer, it is discovered that as Thermal Grashof number increases in Fig. 3, the fluid velocity increases. This result is in line with Bunonyo et al. [12], Prakash et al. [20], Makinde and Chinyoka [21].

Fig. 4 illustrates the outcome of solutal Grashof number on the fluid velocity distribution. As the solutal Grashof number rises the fluid velocity decreases. Also, at any particular value of solutal Grashof number , flow velocity generally decreases towards the boundary wall. The result indicates that at higher value of solutal Grashof number the lesser the flow velocity. The finding is in agreement with Idowu et al. [22].

Fig. 5 shows the influence of magnetic field on the velocity profile. It is discovered that increase in magnetic field decreases the fluid velocity. This is due to Lorentz force which causes a drag in the flow as magnetic field increases. This is in agreement with the work of Nwaigwe [17].

For the case of Fig. 6 the effect of thermal conductivity parameter on fluid temperature is shown, it is seen that as thermal conductivity parameter increases, fluid temperature increases. It is agreement with the work of Idowu et al. [22].

As the heat sink parameter increases in Fig. 7, the fluid temperature decreases. This is physically true when heat is taken away from a system, this is due to boundary layer thickness. See (Nwaigwe and Amadi [18].

Fig. 8 shows the effect of mass diffusive parameter on fluid concentration and it is discovered that as the diffusive parameter increases the fluid concentration decreases. This is physically true that concentration reduces with increase in the rate of diffusion.

The more the solute injection parameter increases the more the increase in fluid concentration in Fig. 9 see also the work of Nwaigwe and Amadi [18].

6 Conclusion

Having studied the effect of mass concentration on a non-isothermal cylindrical channel flow the following conclusions are drawn:

- Increase in viscous parameter decreases flow velocity.
- Flow velocity reduces with increase in magnetic field parameter.
- Increase in Thermal Grashof number increases velocity profile.
- Increase in Thermal Conductivity parameter increases fluid temperature .
- Increase in Mass Diffusivity parameter decreases concentration

Further works can be done by considering multi-directions flow, vertical channel and different flow type such as compressible or inviscid flow.

Competing Interests

Authors have declared that no competing interests exist.

References

[1] Leslie GA, Wilson SK, Duffy BR. Non-isothermal flow of a thin film of fluid with temperature-dependent viscosity on a stationary horizontal cylinder. Physics of Fluids. 2011;23(6):062101.

[2] Nwaigwe, Chinedu, Oluwole Daniel Makinde. Finite difference investigation of a polluted non-isothermal variable-viscosity porous media flow. In Diffusion Foundations. Trans Tech Publications Ltd. 2020;26:145-156.

[3] Nwaigwe, Chinedu, Azubuike Weli, Oluwole Daniel Makinde. Computational analysis of porous channel flow with cross-diffusion. American Journal of Computational and Applied Mathematics. 2019;9(5):119-132.

[4] Conlisk AT, Jie Mao. Nonisothermal absorption on a horizontal cylindrical tube—1. The film flow. Chemical Engineering Science. 1996;51(8):1275-1285.

[5] Duffy BR, Wilson SK. A rivulet of perfectly wetting fluid with temperature-dependent viscosity draining down a uniformly heated or cooled slowly varying substrate. Physics of Fluids. 2003;15(10):3236-3239.

[6] Pinarbasi, Ahmet, Muharrem Imal. Nonisothermal channel flow of a non-Newtonian fluid with viscous heating. International Communications in Heat and Mass Transfer. 2002;29(8).

[7] Adegbie KS, Alao FI. Flow of a Newtonian fluid in a symmetrically heated channel: effect of viscosity and viscous dissipation. Mathematical Problems in Engineering. 2006;2006.

[8] Sahu, Kirti Chandra, Ding H, Matar OK. Numerical simulation of non-isothermal pressure-driven miscible channel flow with viscous heating. Chemical Engineering Science. 2010;65(10):3260-3267.

[9] Jaszczur M, Numerical analysis of a fully developed non-isothermal particle-laden turbulent channel flow. Archives of Mechanics. 2011;63(1):77-91.

[10] Sreenivasulu P, Bhaskar Reddy N. Thermo-diffusion and diffusion-thermo effects on MHD boundary layer flow past an exponential stretching sheet with thermal radiation and viscous dissipation. Advances in Applied Science Research. 2012;3(6):3890-3901.

[11] Ahmed, Sahin G, Hazarika C, Geeti Gogoi. Investigation of variable viscosity and thermal conductivity on MHD mass transfer flow problem over a moving non-isothermal vertical plate. Journal of Naval Architecture and Marine Engineering. 2020;17(2):183-197.

[12] Bunonyo KW, Israel-Cookey C, Amos E. MHD oscillatory flow of jeffrey fluid in an indented artery with heat source. Asian Research Journal of Mathematics. 2017;1-13.

[13] Misyura SY. Non-isothermal evaporation in a sessile droplet of water-salt solution. International Journal of Thermal Sciences. 2018;124:76-84.

[14] Dos Santos, Gabriel Machado, Ítalo Augusto Magalhães de Ávila, Hélio Ribeiro Neto, João Marcelo Vedovoto. Study of non-isothermal two-dimensional flow over a square cylinder immersed in a channel. 25th ABCM International Congress of Mechanical Engineering. Uberlanda, MG, Bzil; October 20-25, 2019.

[15] Nwaigwe C, Ndu RI, Weli A. Wall motion effects on channel flow with temperature-dependent transport properties. Applied Mathematics. 2019;9(3):162-168.

[16] Bunonyo, Kubugha Wilcox, Emeka Amos. Lipid concentration effect on blood flow through an inclined arterial channel with magnetic field. Mathematical modelling and Applications. 2020;5(3):129.

[17] Nwaigwe, Chinedu. Sequential implicit numerical scheme for pollutant and heat transport in a plane-poiseuille flow. Journal of applied and Computational Mechanics. 2020;6(1):13-25.

[18] Nwaigwe, Chinedu, Innocent Uchenna Amadi. Analytical solution of a non-isothermal flow in cylindrical geometry. Asian Research Journal of Mathematics. 2021;17(3):55-76.

[19] Salahuddin T, Mair Khan, Tareq Saeed, Muhammad Ibrahim, Yu-Ming Chu. Induced MHD impact on exponentially varying viscosity of Williamson fluid flow with variable conductivity and diffusivity. Case Studies in Thermal Engineering. 2021;25:100895.

[20] Prakash OM, Makinde OD, Devendra Kumar, Dwivedi YK. Heat transfer to MHD oscillatory dusty fluid flow in a channel filled with a porous medium. Sadhana. 2015;40(4):1273-1282.

[21] Makinde, Oluwole D, Tiri Chinyoka. Numerical investigation of transient heat transfer to hydromagnetic channel flow with radiative heat and convective cooling. Communications in Nonlinear Science and Numerical Simulation. 2010;15(12):3919-3930.

[22] Idowu AS, Jimoh A, Ahmed LO. Impact of heat and mass transfer on MHD oscillatory flow of Jeffery fluid in a porous channel with thermal conductivity, Dufour and Soret. Journal of Applied Sciences and Environmental Management. 2015;19(4):819-830.

Appendix

$$a_2 = \frac{M^2 a_0}{\mu(m+2)^2}; \qquad a_4 = \frac{M^4 a_0}{\mu^2 (m+2)^2 (m+4)^2}; \qquad a_6 = \frac{M^6 a_0}{\mu^3 (m+2)^2 (m+4)^2 (m+6)^2}$$

$$a_8 = \frac{M^8 a_0}{\mu^4 (m+2)^2 (m+4)^2 (m+6)^2 (m+8)^2}; \; a_{10} = \frac{M^{10} a_0}{\mu^5 (m+2)^2 (m+4)^2 (m+6)^2 (m+8)^2 (m+10)^2}$$

$$\dot{a}_2 = \frac{\lambda^2 \dot{a}_0}{\kappa(m+2)^2}; \qquad \dot{a}_4 = \frac{\lambda^4 \dot{a}_0}{\kappa^2 (m+2)^2 (m+4)^2}; \qquad \dot{a}_6 = \frac{\lambda^6 \dot{a}_0}{\kappa^3 (m+2)^2 (m+4)^2 (m+6)^2}$$

$$\dot{a}_8 = \frac{\lambda^8 \dot{a}_0}{\kappa^4 (m+2)^2 (m+4)^2 (m+6)^2 (m+8)^2}; \; \dot{a}_{10} = \frac{\lambda^{10} \dot{a}_0}{\kappa^5 (m+2)^2 (m+4)^2 (m+6)^2 (m+8)^2 (m+10)^2}$$

$$\ddot{a}_2 = -\frac{\alpha^2 \ddot{a}_0}{D(m+2)^2}; \qquad \ddot{a}_4 = \frac{\alpha^4 \ddot{a}_0}{D^2 (m+2)^2 (m+4)^2}; \qquad \ddot{a}_6 = -\frac{\alpha^6 \ddot{a}_0}{D^3 (m+2)^2 (m+4)^2 (m+6)^2}$$

$$\ddot{a}_8 = \frac{\alpha^8 \ddot{a}_0}{D^4 (m+2)^2 (m+4)^2 (m+6)^2 (m+8)^2}; \; \ddot{a}_{10} = -\frac{\alpha^{10} \ddot{a}_0}{D^5 (m+2)^2 (m+4)^2 (m+6)^2 (m+8)^2 (m+10)^2}$$

$$a_1 = a_3 = a_5 = a_7 = a_9 = 0; \qquad \dot{a}_1 = \dot{a}_3 = \dot{a}_5 = \dot{a}_7 = \dot{a}_9 = 0; \qquad \ddot{a}_1 = \ddot{a}_3 = \ddot{a}_5 = \ddot{a}_7 = \ddot{a}_9 = 0$$

$$B_{10} = \frac{1}{M^2}\left(Gr \frac{\theta_w}{\theta_0(1)} \frac{\lambda^{10}}{(2.4.6.8.10)^2.\kappa^5} + Gc \frac{C_w}{C_0(1)} \frac{\alpha^{10}}{(2.4.6.8.10)^2.D^5} \right)$$

$$B_8 = \frac{1}{M^2}\left(Gr \frac{\theta_w}{\theta_0(1)} \frac{\lambda^8}{(2.4.6.8)^2.\kappa^4} - Gc \frac{C_w}{C_0(1)} \frac{\alpha^8}{(2.4.6.8)^2.D^4} + 10^2 \mu B_{10} \right)$$

$$B_6 = \frac{1}{M^2}\left(Gr \frac{\theta_w}{\theta_0(1)} \frac{\lambda^6}{(2.4.6)^2.\kappa^3} + Gc \frac{C_w}{C_0(1)} \frac{\alpha^6}{(2.4.6)^2.D^3} + 8^2 \mu B_8 \right)$$

$$B_4 = \frac{1}{M^2}\left(Gr \frac{\theta_w}{\theta_0(1)} \frac{\lambda^4}{(2.4.\kappa)^2} - Gc \frac{C_w}{C_0(1)} \frac{\alpha^4}{(2.4.D)^2} + 6^2 \mu B_6 \right)$$

$$B_2 = \frac{1}{M^2}\left(Gr \frac{\theta_w}{\theta_0(1)} \frac{\lambda^2}{2^2.\kappa} - Gc \frac{C_w}{C_0(1)} \frac{\alpha^2}{2^2.D} + 4^2 \mu B_4 \right);$$

$$B_0 = \frac{1}{M^2}\left(-p + Gr\frac{\theta_w}{\theta_0(1)} - Gc\frac{C_w}{C_0(1)} + 2^2\mu B_2\right) \quad ;$$

$$A_0 = \frac{-(B_0 + B_2 + B_4 + B_6 + B_8 + B_{10})}{1 + \frac{M^2}{2^2\mu} + \frac{M^4}{(2.4.\mu)^2} + \frac{M^6}{(2.4.6)^2\mu^3} + \frac{M^8}{(2.4.6.8)^2\mu^4} + \frac{M^{10}}{(2.4.6.8.10)^2\mu^5} + \ldots}$$

$$A_2 = \frac{\theta_w}{\theta_0(1)}; \qquad \theta_0(1) = 1 + \frac{\lambda^2}{2^2\kappa} + \frac{\lambda^4}{(2.4.\kappa)^2} + \frac{\lambda^6}{(2.4.6)^2\kappa^3} + \frac{\lambda^8}{(2.4.6.8)^2\kappa^4} + \frac{\lambda^8}{(2.4.6.8.10)^2\kappa^5} + \ldots$$

$$A_4 = \frac{C_w}{C_0(1)}; \; C_0(1) = 1 - \frac{\alpha^2}{2^2 D} + \frac{\alpha^4}{(2.4.D)^2} - \frac{\alpha^6}{(2.4.6)^2 D^3} + \frac{\alpha^8}{(2.4.6.8)^2 D^4} - \frac{\alpha^{10}}{(2.4.6.8.10)^2 D^5} + \ldots$$

Peer-review history:
The peer review history for this paper can be accessed here (Please copy paste the total link in your browser address bar)
https://www.sdiarticle5.com/review-history/95988